CHAPTER VI

EPOXIDIZED NATURAL RUBBER BIO-NANOCOMPOSITE: A MODEL CASE OF BIO-NANOCOMPOSITE USING NANOFIBROUS CHITOSAN AND ITS CONSEQUENT FUNCTIONAL PROPERTIES

6.1 Abstract

A bio-nanocomposite of epoxidized natural rubber with nanofibrous chitosan is proposed. The bio-nanocomposite is formed under the reaction between epoxy groups of ENR and amino and hydroxyl groups of chitosan as confirmed by quali/ quantitative FTIR technique. The nanofibrous chitosan induces the stiffness at nano-scale as observed by AFM and the tensile strength at micro-scale to the ENR-chitosan nanocomposite system. The nanocomposite also performs the copper ion absorptivity as investigated by SEM metal ion mapping mode.

6.2 Introduction

Chitosan (Figure 1a) is the second-most naturally abundant polysaccharide with wide range applications based on bio-related specific properties, metal ion chelation and absorptivity (e.g. Cu^{2+}, Cd^{2+}, and Ni^{2+})[1,2], including the possibility of derivatization. This polysaccharide was reported for its various morphologies such as fibers[3], whiskers[4-6], and nanoparticles[7], etc. In the past, natural rubber nanocomposite with nano-whiskered chitin showing an increase in mechanical property was reported.[4] We found that by simply reprecipitating chitosan acetic acid solution in basic solvent in dilute condition, nano-network fibrous chitosan having diameter in the range of 30-70 nm could be easily obtained as confirmed by TEM (Figure 1b).

Although rubbers are known as thermal and electrical insulator materials, an addition of conductive fillers, such as metal particles, carbon black, and graphite powder[8], enables rubber composites with electrical conductivity for specific applications such as gaskets, keypads, and sensing devices.[9] Epoxidized natural rubber (ENR) (Figure 1c) has a reactive epoxy group to possibly form covalent bonds with chitosan (Figure 1d). The present work, thus, focuses on bio-

nanocomposite system of nanofibrous chitosan and ENR matrices. The fact that (i) chitosan is a light weight material as compared to the traditional fillers mentioned above and (ii) chitosan chelates with various metal ions, the success of ENR-nanofibrous chitosan bio-nanocomposite might lead to novel functional ENR products.

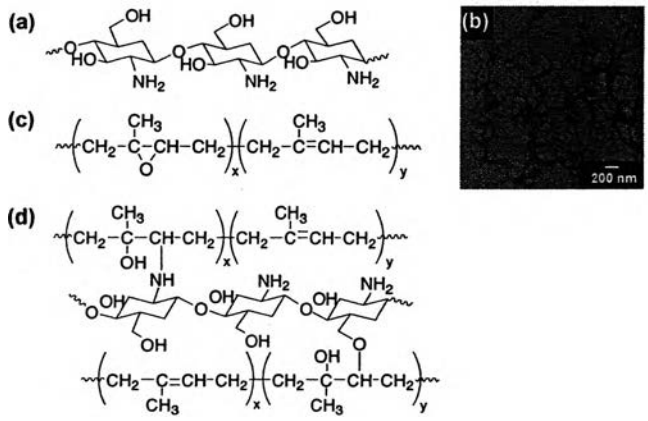

Figure 6.1. Chemical structures of (a) chitosan, and (c) ENR rubber, (d) possible ENR-nanofibrous chitosan bio-nanocomposite structure, and (b) TEM micrograph of reprecipitated showing nanofibrous form.

6.3 Experimental

ENR latex was mixed with nanofibrous chitosan for 2.5, 5, 10, and 20 phr. Each mixture was cast on plastic mold and dried in oven at 60°C to obtain dry sheets before blending with 3, 1.5, 1, and 2 phr of zinc oxide (ZnO), sulfur (S), *N*-cyclohexyl-2-benzothiazyl sulphenamide (CBS), and stearic acid, using a Labtech two roll mills at 40°C. The ENR and ENR-chitosan nanocomposites were vulcanized by a Vantage compression molding at 150°C for the optimum cure time (t_{90}) as determined by a Rheotch MD+ moving die rheometer (MDR).

6.4 Results and disscussion

In order to identify the structure as shown in Figure 1d, quali/quantitative FTIR analyses were carried out.[10] Figure 2A shows an example of ENR-nanofibrous chitosan bio-nanocomposite as compared to those of ENR and chitosan. The curve

fittings in the range of 3000-2700 cm^{-1} for methyl group in ENR (CH_3 stretching) and of 920-770 cm^{-1} for epoxy group (C–O–C bending) were done to trace how epoxy group was changed (Figure 2B). The quantitative analysis of epoxy group based on ν_{as} and ν_s of CH_3 group at 2960 cm^{-1} and 2925 cm^{-1} (Figure 2C) shows the amount of epoxy group is reduced significantly at the blend system with chitosan content 2.5 phr and is continuously decreased for chitosan content from 5 to 20 phr. This implies a reactive blending of ENR-nanofibrous chitosan during bio-nanocomposite formation.

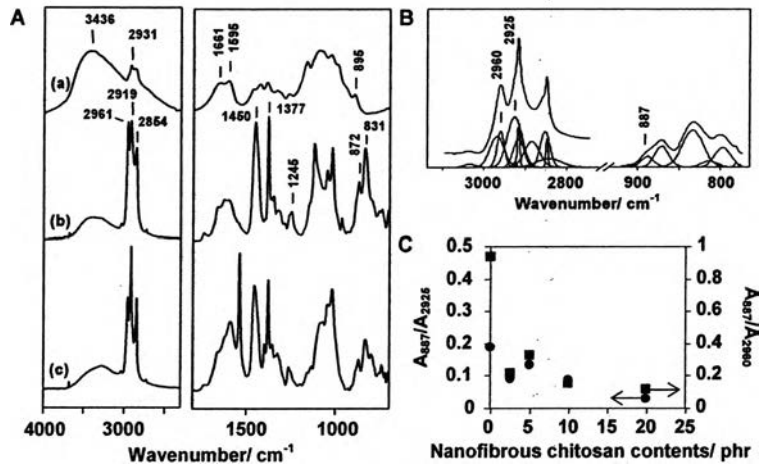

Figure 6.2. (A) FTIR spectra of (a) nanofibrous chitosan, (b) ENR, and (c) ENR-nanofibrous chitosan bio-nanocomposite (10 phr), (B) curve fitting of ENR-nanofibrous chitosan bio-nanocomposite (10 phr), and (C) quantitative analysis based on (B) at various chitosan contents.

In order to evaluate the effect of nanofibrous chitosan on the surface property of ENR, NR latex was used as a reference by coating NR on both ENR and ENR-nanofibrous chitosan bio-nanocomposites sample surfaces. Figure 3A shows topographic atomic force microscopy (AFM) images. As compared to the pure ENR, ENR-nanofibrous chitosan bio-nanocomposite displays the rough surface. This implies the existence of nanofibrous chitosan on the surface and the consequent roughness (the circular area in Figure 3A(b)). Figures 3B and 3C are the FMM amplitude images and profiles. The pure ENR surface shows the dark area (Figure 3B(a)) with a low signal in amplitude profile (Figure 3C(a)). By comparing these

results with those of NR reference, it is clear that the ENR surface is softer than that of NR. However, ENR-nanofibrous chitosan bio-nanocomposite displays a light image (Figure 3B(b)) and a high amplitude profile signal (Figure 3C(b)) as compared to ENR. This implies that the nanofibrous chitosan initiates stiffness onto ENR surface. Bar et al. demonstrated the similar FMM result for alkanethiols[11] to conclude the stiffness of the material.

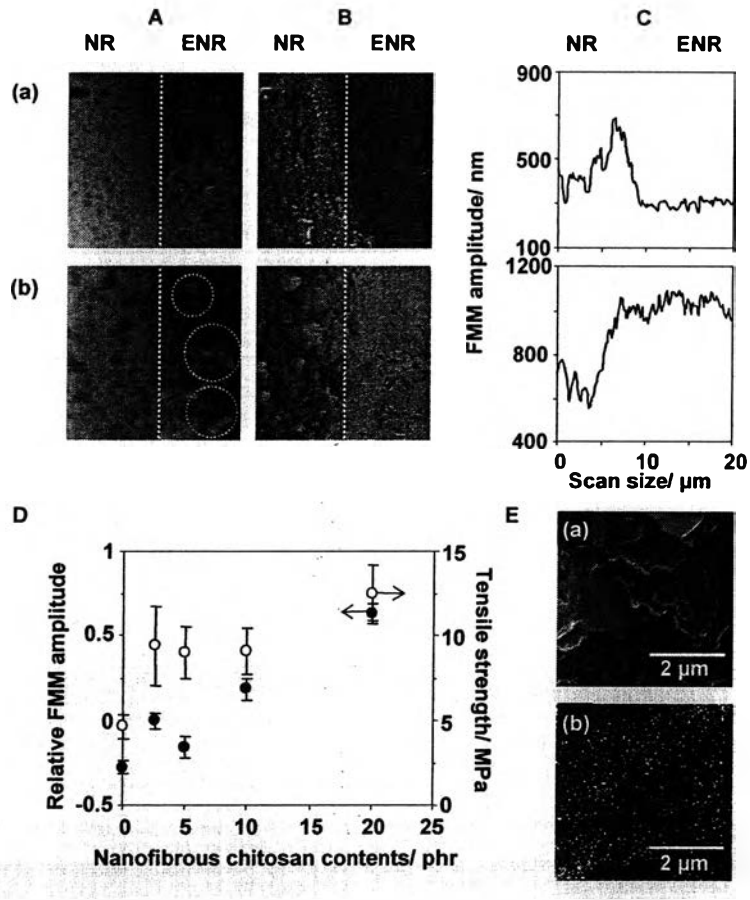

Figure 6.3. (A) Topographic AFM images, (B) FMM amplitude AFM images (20 μm^2), (C) FMM amplitude profiles of; (a) ENR and (b) ENR-nanofibrous chitosan bio-nanocomposite (20 phr), (D) relative FMM amplitude (●) and tensile strength (○) of ENR-nanofibrous chitosan bio-nanocomposite with various chitosan contents, and (E) FE-SEM micrographs of ENR-nanofibrous chitosan bio-nanocomposite (20 phr) after immersing in copper sulfate solution: (a) surface and (b) mapping mode (Note: For (A), (B), and (C), a reference NR was shown in the left area).

The relative FMM amplitudes were evaluated using NR as a reference and were plotted against nanofibrous chitosan contents to evaluate the changes of the surface stiffness of the ENR-nanofibrous chitosan bio-nanocomposite (Figure 3D). The FMM amplitude increases almost linearly with an increase of nanofibrous chitosan contents which confirms the surface stiffness enhanced after adding nanofibrous chitosan.

The pure ENR shows the smooth surface whereas the ENR-nanofibrous chitosan bio-nanocomposite shows the rough one (Figure 3E(a)) as observed by field emission scanning electron microscope (FE-SEM) technique, which is relevant to the topographic AFM image (Figure 3A(b)). This confirms that the nanofibrous chitosan induces the rough surface to ENR. Considering the specific property of chitosan related to the metal chelation, an immersion of ENR and ENR-nanofibrous chitosan bio-nanocomposite in the metal ion solution for overnight was carried out. Figure 3E(b) displays the surfaces of ENR-nanofibrous chitosan bio-nanocomposite after immersing in copper sulfate solution (2%, w/v) using copper ion FE-SEM mapping mode. The result clearly shows the copper distribution on the bio-nanocomposite surface. This reflects the function of amino group in copper absorption.[1,2]

It comes to the question that how those nano-scale and micro-scale induces the changes in millimeter scale. The ENR and ENR-nanofibrous chitosan bio-nanocomposite were compressed in a sheet form to evaluate the tensile strength. Figure 3D shows the plot of ENR with various nanofibrous chitosan contents to find that the tensile strength increases with an increase of chitosan content. With only 5 phr content of nanofibrous chitosan, the tensile strength is significantly increased for two times. The result was relevant to the surface stiffness in nano-scale as plotted by relative FMM amplitude.

6.5 Conclusion

The epoxy group of ENR allowed a reactive blend in the obtaining ENR-nanofibrous chitosan bio-nanocomposites. The nanocomposites showed an enhancement in surface roughness and stiffness, an increase in tensile strength, and a metal ion absorptivity, therefore; this bio-nanocomposite can be expected for a novel ENR functional material.

6.6 Acknownledgement

The present work was supported by SRI R&D Ltd., Japan. The authors acknowledge Seafresh Chitosan (Lab) Company Limited (Thailand), Sumirubber Malaysia SDN (Malaysia), R&D Center for Thai Rubber Industry (Thailand), Labtech Company Limited (Thailand), and the Hitachi High-Technologies Corporation (Japan).

6.7 References

1 K. Kurita, T. Sannun, Y. Iwakura, *J. Appl. Polym. Sci.* **1979**, 23, 511.

2 F-C. Wu, R-L. Tseng, R-S. Juang, *Ind. Eng. Chem. Res.* **1999**, 38, 270.

3 S. Hirano, K. Nagamura, M. Zhang, S. K. Kim,B. G. Chung, M. Yoshikawa, T. Midorikawa, *Carbohydr. Polym.* **1999**, 38, 293.

4 a) K. G. Nair, A. Dufresne, *Biomacromolecules* **2003**, 4, 657. b) K. G. Nair, A. Dufresne, *Biomacromolecules* **2003**, 4, 666.

5 S. Phongying, S-I. Aiba, S. Chirachanchai, *Polymer* **2007**, 48, 393.

6 T. Lertwattanaseri, N. Ichikawa, T. Mizoguchi, Y. Tanaka, S. Chirachanchai, *Carbohyd. Res.* **2009**, 344, 331.

7 R. Yoksan, M. Akashi, K. Hiwatari, S. Chirachanchai, *Biopolymers.* **2003**, *69*, 386.

8 D-Y. Jeong, J. Ryu, Y-S. Lim, S. Dong, D-S. Park. *Sensor. Actuat. A-Phys.* **2009**, 149, 246.

9 A. M. Shanmugharaj, J. H. Bae, K. Y. Lee, W. H. Noh, S. H. Lee, S. H. Ryu, *Compos. Sci. Technol.* **2007**, 67, 1813.

10 Chitosan, FTIR (cm^{-1}): 3500–3300 (OH), 3000–2800 (C–H stretching), 1661 (amide I), and 1595 ($–NH_2$); ENR, FTIR (cm^{-1}): 2961, 2919, and 2854 (C–H stretching), 1450 (C–H bending of $–CH_2–$), 1377 (C–H bending of $–CH_3$), 870 (C–O–C bending of epoxy group), and 836 (C–H bending of C=C–H).

11 G. Bar, S. Rubin, A. N. Parikh, B. I. Swanson, T. A. Zawodzinski, *Langmuir* **1997**, 13, 373.